An FLIR Video Surveillance System to Avoid Bridge-Ship Collision

Jun Liu, Hong Wei, Xi-Yue Huang, Nai-Shuai He and Ke Li

***Abstract*—In this paper, a forward-looking infrared (FLIR) video surveillance system is presented for collision avoidance of moving ships to bridge piers. An image pre-processing algorithm is proposed to reduce clutter noises by multi-scale fractal analysis, in which the blanket method is used for fractal feature computation. Then, the moving ship detection algorithm is developed from image differentials of the fractal feature in the region of surveillance between regularly interval frames. Experimental results have shown that the approach is feasible and effective. It has achieved real-time and reliable alert to avoid collisions of moving ships to bridge piers.**

***Index Terms*—Bridge-ship collision avoidance, infrared image, fractal, moving target detection.**

I. INTRODUCTION

THE fact that more and more ships are built while their size becomes bigger and bigger is introducing the high risk of collision between bridge and ship in inland waterways. Incidences of ship-bridge collision mainly cause six types of results, *i.e.* damage of bridge, people casualty, damage of ship and goods, economical loss, social loss and environmental loss. A large amount of statistical analysis indicates that one of main reasons resulting in ship-bridge collision is the execrable natural environment such as poorly visible conditions and floods etc [1-2].

Mainly, there are two existing strategies to avoid bridge-ship collision at present [3-4]. One is the passive strategy in which fixed islands or safeguard surroundings are built around bridge piers. The shortages of the passive method are: it could not avoid ship damage from a collision; the costs are normally high; and it becomes less effective with constant increase of ship size. The other is the active strategy which uses radar or video images to monitor moving ships by measuring their course for collision estimation. Compared with the passive method, the active method avoids damage of both bridge and ship and its costs are low. However radar is difficult to detect course changes immediately due to its low short-term accuracy, and the high noise level makes radar sometimes hardly detect any objects from a clutter background. Sensors for visible light do not work well under poorly illuminated conditions such as fog, mist and night. In contrast, infrared sensors are capable of adapting weather and light changes during a day. Especially, the FLIR images can overcome the problems that radar has, *i.e.* they have high short-term angle accuracy.

In design, the first consideration of the FLIR surveillance system is its robustness for detecting moving ships. The main difficulties are: 1) low thermal contrast between the detected object and its surroundings; 2) relatively low signal to noise ratio (*SNR*) under the weak thermal contrast; and 3) insufficient geometric, spatial distribution and statistical information for small targets [5].

Motion detection in a surveillance video sequence captured by a fixed camera can be achieved by many existing algorithms, *e.g.* frame difference, background estimation, optical flow method, and statistical learning method [6]. The most common method is the frame difference method for the reason that it has a great detection speed and low computation cost. However the detection accuracy by using this method is strongly affected by background lighting variation between frames. The most complex algorithm is the optical flow method, by which the computation cost is high. The statistical learning method needs training samples which may not be available in most cases, and its computation cost is also relatively high. These two methods are not suitable for real-time processing. The background estimation method is extremely sensitive to the changes of the lighting condition in which the background is established.

In the FLIR surveillance video sequence used for moving ship detection, a background normally consists of various information, such as sky, the surface of river, water waves, and large floating objects (non-detected objects) in a flooding season, etc. In many cases, ships and background in FLIR images are visually merged together. It is very difficult to detect the targets (moving ships) using normal methods mentioned above.

The new FLIR video surveillance system for bridge-ship collision avoidance is proposed in Section II. Section III presents the novel infrared image pre-processing algorithm using multi-scale fractal analysis based on the blanket method. The moving ships detection algorithm in the region of surveillance is developed in Section III, too. Section IV demonstrates the experimental results that are discussed and analyzed in details. Finally, conclusions and future work are presented in Section V.

II. THE FLIR VIDEO SURVEILLANCE SYSTEM

In the system, a pan-tilt is fixed on bridge pier, and FLIR camera is installed on the pan-tilt. The visual region of FLIR *i.e.* the region of surveillance, can be adjusted by the pan-tilt, and is configured according to real conditions. The FLIR camera links to a personal computer (*PC*) through a frame grabber. When images are captured, the image processing program in *PC*'s memory is used to detect the moving ships. When the moving ships are detected in region of surveillance, the device for safety alert is started. The ship driver could be

Manuscript received March 2, 2008. This research is partially supported by the China Scholarship Council (CSC).

J. Liu, X. Y. Huang, N. S. He and K. Li are with the Navigation & Guidance Lab, College of Automation, University of Chongqing, Chongqing, 400030, CHINA (e-mail: gutlj@163.com, xyhuang@cqu.edu.cn, hns2002@163.com, likelinqiu@163.com).

H. Wei is with the Computational Vision Lab, School of Systems Engineering, University of Reading, Reading, RG6 6AY, UK (e-mail: h.wei@reading.ac.uk).

alarmed if necessary, and he/she would take maneuvers to avoid ship-bridge collision. The flowchart of the system is depicted in Fig. 1.

A large amount of experiments carried out in the Changjiang River have proved that the minimum pre-warning distance between bridge pier and ship to avoid collision is 500m in inland waterway, and the valid distance for moving ship detection is from 800m to 2000m when the uncooled infrared focal plane arrays (*FPA*) thermal imaging camera is used. Therefore, this type of camera is suitable for the application. The resolution is 320×240 pixels. There are three ways designed to trigger the pre-warning signal, *i.e.* automatically broadcast the pre-recorded voice through very high frequency (*VHF*) or loudspeaker, or automatically turn on the assistant lighting system.

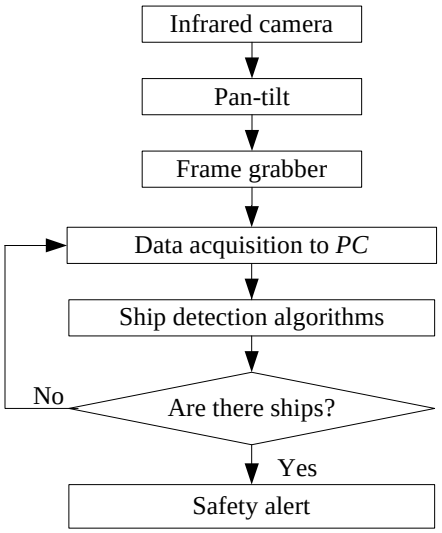

Fig. 1. Flowchart of the system framework

III. THE DETECTION ALGORITHM FOR MOVING SHIPS

In order to detect moving ships in an FLIR image from complicated background along the inland waterway, a novel detection algorithm is developed. It consists of four main stages: extracting the region of interest, *i.e.* the region of surveillance (*ROS*); calculating the multi-scale fractal feature; generating the binary image based on the fractal feature; detecting moving ships by a frame difference method. The algorithm is schematically demonstrated in Fig. 2.

A. Extracting the ROS

The *ROS* is defined based on various conditions in real parts of the inland waterway. Consequently, the *ROS* appears as a part of region in the original image. The image analysis and processing is focused on the region only. This excludes the unwanted regions to reduce computation cost for further processing.

B. Calculating the Multi-scale Fractal Feature

In practice, ships in FLIR images are treated as man-made objects in contrast to natural background. A fractal model can well describe complex surface structure characteristics for natural objects, but not for man-made objects [7-8]. To some extent, fractal features of natural background keep relatively stable, but fractal features of man-made objects behave obviously variety. Therefore, the fluctuation of fractal features distinguishes natural and man-made objects along with the variation of scale. The multi-scale fractal feature is proposed to reduce interference of natural background and enhance the intensity of ships.

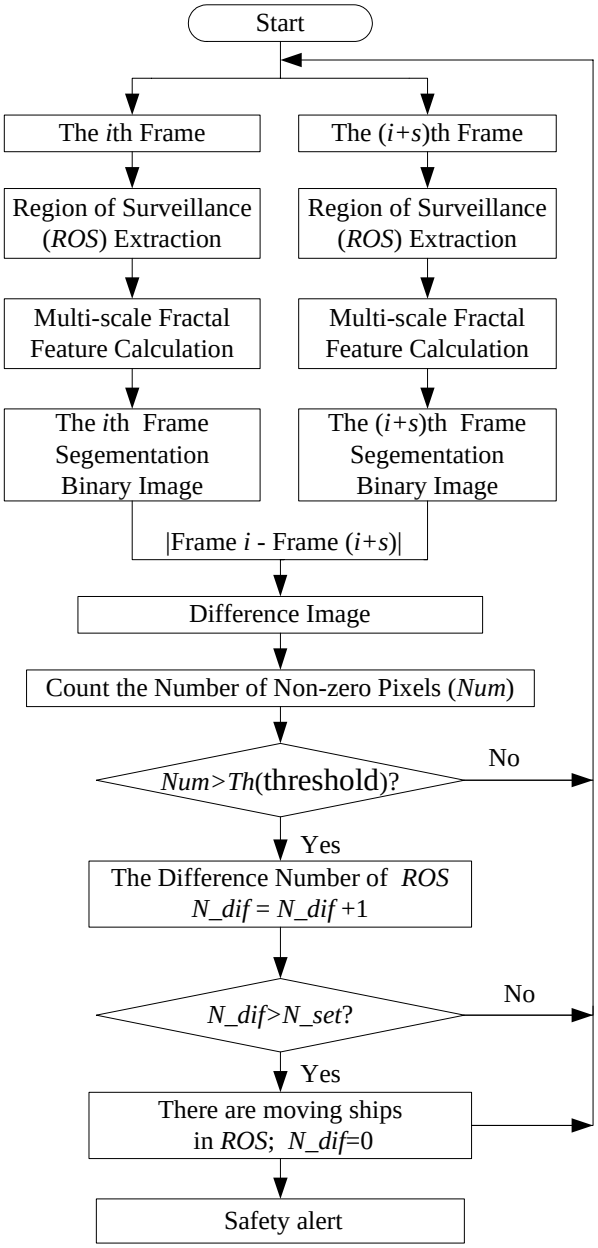

Fig. 2. The detection algorithm

Many researchers [9-10] adopted Mandelbrot's idea and extended it to surface area calculation. For a grey image surface, the fractal dimension can be estimated as in (1).

$$A(\varepsilon) = K\varepsilon^{2-D} \tag{1}$$

where D is the fractal dimension, K is a constant, ε is the scale with value of $0,1,\cdots,\varepsilon_{\max}$, and $A(\varepsilon)$ is the surface area of image in the scale ε.

Let $f(x,y)$ a grey image, the image could be viewed as a hilly terrain surface whose height from the normal ground is proportional to the image grey value. Then all points at

distance ε from the surface on both sides create a blanket of thickness 2ε. The estimated surface area is the volume of the blanket divided by 2ε. For different scale ε ($\varepsilon \geq 0$), the blanket area can be iteratively estimated. The upper surface $u(x, y, \varepsilon)$ and the lower surface $b(x, y, \varepsilon)$ are expressed in (2) and (3), respectively.

$$u(x, y, 0) = b(x, y, 0) = f(x, y) \qquad \varepsilon = 0$$
$$u(x, y, \varepsilon) = \max\{u(x, y, \varepsilon - 1), \max_{|(m,n)-(x,y)| \leq 1} u(m, n, \varepsilon - 1)\} \quad (2)$$
$$b(x, y, \varepsilon) = \min\{b(x, y, \varepsilon - 1), \min_{|(m,n)-(x,y)| \leq 1} b(m, n, \varepsilon - 1)\} \quad (3)$$
$$\varepsilon = 1, 2, \cdots, \varepsilon_{\max}$$

where, the image points (m, n) with distance less than one from (x, y) is the four neighbors of (x, y). To assure the blanket of the surface for scale ε includes all the points of the blanket for scale $\varepsilon - 1$, (m, n) are chosen to be the eight neighbors of pixel (x, y) in the experiments.

$\varepsilon_{\max}$ is the maximum scale when the fractal features are calculated. $\varepsilon_{\max} \in N, \varepsilon_{\max} \geq 2$.

At scale ε, the volume between the upper surface and the lower surface is calculated by (4):

$$V(x, y, \varepsilon) = \sum_{k=x-\varepsilon}^{x+\varepsilon} \sum_{m=y-\varepsilon}^{y+\varepsilon} [u(k, m, \varepsilon) - b(k, m, \varepsilon)] \quad (4)$$

Then, the estimate of the surface area at (x, y) and ε can be obtained by (5):

$$A(x, y, \varepsilon) = \frac{V(x, y, \varepsilon)}{2\varepsilon} \quad (5)$$

Taking the logarithm of both sides in (1), we have:

$$\log A(x, y, \varepsilon) = (2 - D)\log(\varepsilon) + \log K \quad (6)$$

Linearly fitting $\log A(x, y, \varepsilon)$ against scale ε in (6), fractal dimension D can be obtained as a constant for all scales ε.

For the constant K in (1), also named *D-dimensional area* [2], which characterizes the roughness of surface, *i.e.* different surfaces have different K values. From this point of view, K is not a constant for the variation of scale. When two scales ε_1, ε_2 are used in (6), we have:

$$\log A(x, y, \varepsilon_1) = (2 - D)\log(\varepsilon_1) + \log K \quad (7)$$
$$\log A(x, y, \varepsilon_2) = (2 - D)\log(\varepsilon_2) + \log K \quad (8)$$

In (7) and (8), fractal dimension D is a constant for scale ε_1 and ε_2, and let $\varepsilon_1 = \varepsilon, \varepsilon_2 = \varepsilon + 1$, $\varepsilon = 0, 1, 2, \cdots \varepsilon_{\max}$, $K(x, y, \varepsilon)$ is derived as

$$K(x, y, \varepsilon) = \exp\left(\frac{\log A(x, y, \varepsilon)\log(\varepsilon + 1) - \log A(x, y, \varepsilon + 1)\log(\varepsilon)}{\log(\varepsilon + 1) - \log(\varepsilon)}\right) \quad (9)$$

From (9), the *D-dimension area* $K(x, y, \varepsilon)$ can be calculated from surface area $A(x, y, \varepsilon)$ at point (x, y) along with scale ε. We use a new function $C(x, y)$ to measure the deviation of $K(x, y, \varepsilon)$ against scale ε, as presented in (10).

$$C(x, y) = \sum_{\varepsilon=2}^{\varepsilon_{\max}} [K(x, y, \varepsilon) - \frac{1}{\varepsilon_{\max} - 1} \sum_{\varepsilon=2}^{\varepsilon_{\max}} K(x, y, \varepsilon)]^2 \quad (10)$$

$C(x, y)$ is the fractal feature used for ship detection in the algorithm. $C(x, y)$ appears a large value for man-made objects, and a much small value for natural background.

C. Segmenting the Fractal Feature Image

$C(x, y)$ provides sufficient information to discriminate natural background and ships. The simplest *OSTU* segmentation method [11] is used to segment the $C(x, y)$ image. In the resulting binary image, pixel value 255 represents ships and other man-made objects.

D. Detecting moving ships

In the process of moving ship detection, a difference between two binary images generated from segmentation of $C(x, y)$ is used. A group of pixels with none-zero values represent the difference. Based on the fact that the FLIR camera is fixed on bridge pier, it is estimated that moving ships are in the *ROS* if the number of pixels in *ROS* changes persistently. The process is summarized as follows.

1) Generate two binary images $C_i(x, y)$ and $C_{i+s}(x, y)$ by segmentation of two frames with interval of s, $f_i(x, y)$ and $f_{i+s}(x, y)$. In practice, the interval s is chosen as 5 to 10 frames.

2) Calculate the difference between image $C_i(x, y)$ and $C_{i+s}(x, y)$, and obtain $D(x, y)$.

3) To count the number of non-zero pixels in $D(x, y)$, and record it as *Num*.

4) If *Num* is larger than the threshold (*th*) which is experimentally obtained, denote the number of pixels in *ROS* have changed once, then the difference number of *ROS* (*N-dif*) add one.

5) If *N-dif* is larger than a pre-set value *N_set* from experiments, denote that moving ships are detected in the *ROS*. In practice, the value *N_set* is set as 2 or 3, which is effective in reducing the false alarm ratio.

IV. EXPERIMENTAL RESULTS AND DISCUSSION

The testing experiments were carried out in the Changjing River in Chongqing city, China. A FLIR camera was mounted on a bridge pier, a Celeron1.5Ghz PC was connected with the camera through a frame grabber, the frame size was 320×240, and the frame rate was 30 fps. The parameter settings in the algorithm were, the frame interval as 10 frames, the value of threshold (*th*) as 5, the value of *N_set* as 2, and the value of $\varepsilon_{\max}$ as 4. A group of testing results is demonstrated in Fig. 3. The average processing time for each step in the algorithm is shown in Table I.

TABLE I
AVERAGE PROCESSING TIME FOR EACH STEP

Steps	Time (ms)
Extracting the region of surveillance	5
Calculating $C(x, y)$	331
Segmenting $C(x, y)$ image	22
Detecting moving ships based on frame difference	25
Other steps	10
Total	393

TABLE II
COMPARATIVE PERFORANCE ANALYSIS

	Frame difference method	The proposed method
FAR	23.1%	Lower than 1%
MAR	17.6%	Lower than 1%

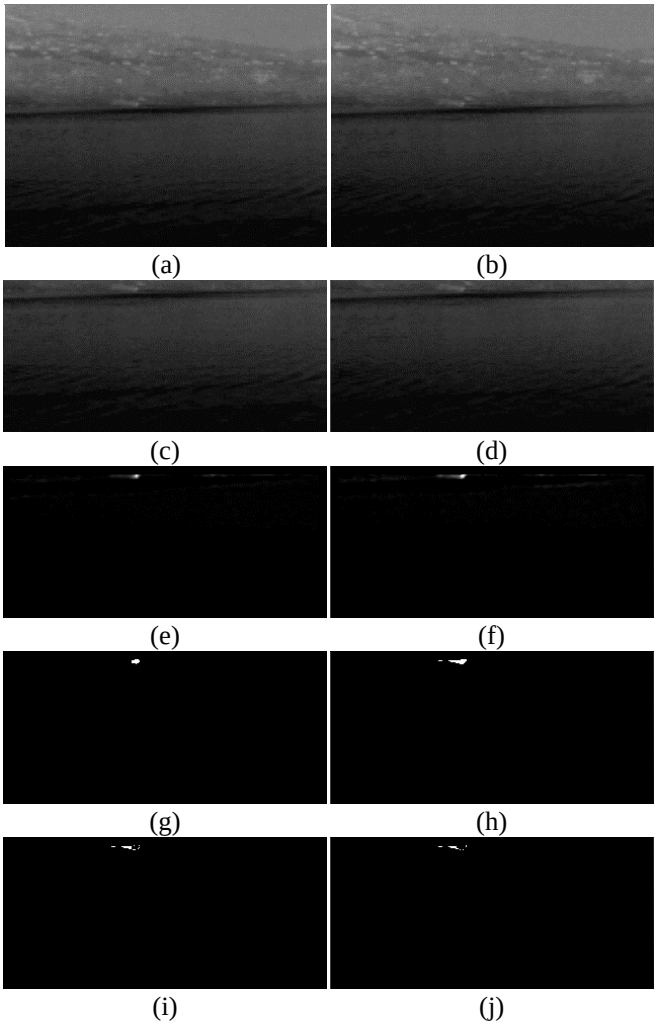

Fig. 3. Testing results. (a) The 1st original frame. (b) The 11th original frame 11th. (c) The *ROS* image extracted from (a). (d) The *ROS* image extracted from (b). (e) $C(x, y)$ of the 1st frame. (f) $C(x, y)$ of the 11th frame. (g) Segmenting binary image from (e). (h) Segmenting binary from (f). (i) $D(x, y)$ between the 11th and the 1st frames, *Num*=32. (j) $D(x, y)$ between the 21st and the 11th frames, *Num*=25.

Observations have indicated that the speed of moving ships is from 20 *km/h* to 30 *km/h*. The *ROS* defines the distance between moving ships and bridge pier as 800*m* to 2000*m*. Therefore the time during which a ship driver takes action to avoid collision to a bridge pier after altered is between 96 seconds and 360 seconds. From Table I, it is clearly shown that the FLIR surveillance system takes about one second to complete a process. It is satisfactory in the application with a real-time manner.

Comparative experiments were also carried out for system performance analysis in terms of reliability and effectiveness. The frame difference method was implemented to be compared with the proposed method. FLIR frames were carefully selected for this comparison. Weather conditions and time of a day were taken into account when 400 frames with 286 moving ships involved were chosen as the testing set. Two parameters were introduced as the criterion for the performance, *i.e.* false alarm ratio (*FAR*) and missed alarm ratio (*MAR*). The comparative results are shown in Table II.

From the results in table II, it can be seen that the proposed method for bridge-ship collision-avoidance is superior to the frame difference method in the criterion of both false alarm ratio and missed alarm ratio.

V. Conclusion

This paper presented a novel FLIR video surveillance system for bridge-ship collision avoidance by using the multi-scale fractal feature, by which moving ships has successfully been separated from the complex background in inland waterway images. The proposed algorithm for moving ship detection has achieved the real-time performance within the *ROS* in FLIR video sequences. Experimental results have proved that the developed FLIR video surveillance system is efficient in detecting moving ships to alert possible bridge-ship collisions. Its wide adaptability and high reliability makes it to be able to work in reality.

Our future work will be extended to two venues. First, the investigation for tracking multiple ships will be carried out based on the ship detection results. Relative tracking algorithms will be developed to address the issue in a clutter background. Second, a data fusion of radar and infrared sensors may be explored to improve system performance in making use of the complement of data from different sensors.

ACKNOWLEDGMENT

The authors would like to thank the Maritime Safety Administration of Chongqing for providing experimental sites.

REFERENCES

[1] T. D. Dai, W. Lie, and W. L. Liu, "The analysis of ship-bridge collision in main waterway of the Yangtze River," *Navigation of China*, vol. 4, pp. 44–47, July 1993.

[2] S. E. Van Manen, "Ship collisions due to the presence of bridge," International Navigatio Association (PIANC), Brussels, Report of WG 19, 2001.

[3] Q. Y. Zhu, "Pier anticollision system based on image processing," Master's thesis, Dept. Information Eng., Wuhan Univ. of Technology, Wuhan, 2006.

[4] J. Wu, "Development of ship-bridge collision analysis," *Journal of Guangdong Communication Polytechinic*, vol. 4, pp. 60–64, April 2004.

[5] J. Liu, X. Y. Huang, Y. Chen, and N. S. He, "Target recognition of FLIR images on radial basis function neural network," in *Proc. Advances in Neural Networks, ISNN 2007, 4th International Symposium on Neural Networks*, Nanjing, 2007, pp. 772–777.

[6] C. H. Zhan, X. H. Duan, S. Y. Xu, Z. Song, and M. Luo, "An improved moving object detection algorithm based on frame difference and edge detection," in *Proc. Fourth International Conference on Image and Graphics*, Chengdu, 2007, pp. 519–523.

[7] B. B. Mandelbrot, *The fractal geometry of nature*. New York: W.H. Freeman, 1982, pp. 1–24.

[8] A. Pentland, “Fractal-based description of natural scenes,” *IEEE Trans. Pattern Analysis and Machine Intelligence*, vol. 6, pp. 661–674, November 1984.
[9] S. Peleg, J. Naor, R. Hartley, and D. Avnir, “Multiple resolution texture analysis and classification,” *IEEE Trans. Pattern Analysis and Machine Intelligence*, vol. 6, pp. 518–523, July 1984.
[10] H. Zhang, X. L. Liu, J. W. Li, and Z. F. Zhu, “The study of detecting for IR weak and small targets based on fractal features,” in Lecture Notes in Computer Science, Advances in Multimedia Modeling. Heidelberg: Springer Berlin, 2006, pp. 296–303.
[11] N. Ostu, “A threshold selection method from gray-level histograms,” *IEEE Trans. System, Man and Cybernetics*, vol. SMC-9, pp. 62–66, January 1979.